Chinese Physics C Vol. 49, No. 9 (2025) 094005

# Constraint on symmetry energy slope using neutron skins of $^{48}$Ca, $^{64}$Ni, $^{124}$Sn, and $^{208}$Pb and its impact on neutron star radius*

Yu Huang (黄宇)[1,2] Kai-Xuan Huang (黄开轩)[3] Zu-Xing Yang (杨祖星)[4] Xiao-Lin Tu (涂小林)[2†] Jin-Niu Hu (胡金牛)[3] Jing-Tao Zhang (张景涛)[2] Ji-Feng Han (韩纪锋)[1]

[1]Key Laboratory of Radiation Physics and Technology of the Ministry of Education, Institute of Nuclear Science and Technology, Sichuan University, Chengdu 610064, China
[2]Institute of Modern Physics, Chinese Academy of Sciences, Lanzhou 730000, China
[3]School of Physics, Nankai University, Tianjin 300071, China
[4]RIKEN Nishina Center, Wako, Saitama 351-0198, Japan

**Abstract:** We constrain the symmetry energy slope $L$ at the saturation density using the neutron skin values of $^{48}$Ca, $^{64}$Ni, $^{124}$Sn, and $^{208}$Pb determined by various experiments. The resulting $L$ of 50(6) MeV is consistent with the world-averaged value from different observables and methodologies. The implications of newly constrained $L$ on the radius determinations of 1.4 solar-mass neutron stars are also discussed based on the established $R_{1.4}$-$L$ linear relationships by the DD-ME2 and TW99 EoS families.

**Keywords:** neutron skin, symmetry energy slope, neutron star radius

**DOI:** 10.1088/1674-1137/add9fd **CSTR:** 32044.14.ChinesePhysicsC.49094005

## I. INTRODUCTION

The equation of state (EoS) of isospin asymmetric nuclear matter plays an important role in research on nuclear reaction and structure as well as astrophysics [1]. For example, bulk properties of neutron stars are mainly governed by the EoS [1−4]. Many investigations indicate that there are significant correlations between neutron star radii and EoS parameters, namely, the symmetry energy slope $L$ at the saturation density $\rho_0$, nuclear matter incompressibility coefficient $K_0$, and skewness parameter $Q_0$ [4−9]. In particular, the radii of neutron stars with density $\rho\sim\rho_0$ are primarily determined by the slope $L$ [4]. These findings are important, and many attempts have been made to precisely determine EoS parameters [7, 10]. $K_0$ was constrained with a precision of approximately 10% to be 240(20) MeV by giant resonance [11, 12], which agrees with recent results [13]. However, the deduced $L$ values at $\rho_0$ by different methodologies have a large spread from approximately 30 to 110 MeV. For more details, see the review article in Ref. [14]. In particular, due to a lack of sensitive observables, $Q_0$ is still poorly understood. Theoretical values for $Q_0$ are in the range of $\sim -1000$ to $\sim 1000$ MeV [15].

Similar to neutron star radii, it is well known that neutron skins formed in heavy nuclei with an excess of neutron over proton are sensitive to the slope $L$ at $\rho_0$ [16]. Because the linear relationships were established based on different effective nucleon-nucleon interactions of the self-consistent mean-field models [16], neutron skin thicknesses $\Delta R_{np}$, as the difference of neutron and proton distribution rms radii in nuclei, namely, $\Delta R_{np}=R_n-R_p$, have been widely employed to constrain the slope $L$. Theoretical progress has also promoted the development of novel experimental methods for neutron distribution radius measurements [17−26]. Recently, model-dependent $\Delta R_{np}$ data for the stable Ca, Ni, Sn, and Pb isotopes were compiled, and the evaluated $\Delta R_{np}$ values showed a high precision of approximately 0.02 fm [27]. These compiled $\Delta R_{np}$ data [27] are taken from different experiments related to hadron scatterings [18, 24, 28], interaction cross sections [25, 29], giant resonances [30, 31], and antiprotonic atoms [22, 32]. Based on the compiled $\Delta R_{np}$ data, separate trends of $\Delta R_{np}$ versus relative neutron excess, $\delta=(N-Z)/A$, were observed for the Ca, Ni, Sn, and Pb isotopic chains [27], where $N$, $Z$, and $A$ reperesent neutron, proton, and mass numbers, respectively. In addition, parity-violating electron scattering provides a so-called mode-independent approach to determine $\Delta R_{np}$ in nuclei [23, 33]. With this method, the $\Delta R_{np}$ of $^{48}$Ca and $^{208}$Pb were determined by the CREX and PREX collaboration groups [23, 33], respectively. Although the tension of the CREX-PREX neutron skins with other experimental and theoretical results has been widely discussed from a phys-

Received 5 March 2025; Accepted 16 May 2025; Published online 17 May 2025
* Supported in part by the National Key R&D Program of China (2023YFA1606401) and by the NSFC (12375115, 12121005)
† E-mail: E-mail: tuxiaolin@impcas.ac.cn

ics perspective [34–37], the possibility of statistical fluctuations was also mentioned in Refs. [38–40]

The $\Delta R_{np}$ data from different experimental methods would be helpful to reduce the model-dependent effects of single experimental data [41]. For instance, using the $\Delta R_{np}$ of Sn isotopes from different experiments, highly precise $L$ values at different densities have already been obtained in Refs. [42, 43]. We note that the compiled neutron skin data from different experimental methods reproduce the separate $\Delta R_{np}$ structures of Ca, Ni, Sn, and Pb isotope chains predicted by the SLy4 interaction [27]. This would indicate that these compiled neutron skin data are reliable. Therefore, it is interesting to precisely constrain the symmetry energy slopes $L$ at the saturation density using the compiled $\Delta R_{np}$ data [27] and to address their impacts on the neutron star radii at 1.4 solar-mass ($1.4\,M_\odot$).

## II. DETERMINATION OF SYMMETRY ENERGY SLOPE

As known, the symmetry energy slope $L$ at the saturation density can be sensitively constrained by the $\Delta R_{np}$ value of heavy nuclei with large neutron-to-proton values [43, 44]. Therefore, for each isotope chain tabulated in Ref. [27], we only adopt the $\Delta R_{np}$ data of magic nucleus with the maximum neutron-to-proton value, namely $^{48}$Ca, $^{64}$Ni, $^{124}$Sn, and $^{208}$Pb, to determine the slope $L$. It would also be helpful to reduce the effects of possible $\Delta R_{np}$ isotope-dependent deviation on the $L$ extraction through balancing the contribution of each isotope chain. To constrain $L$ in this study, the $\Delta R_{np}$ values are analyzed via the chi-square $\chi_j^2$ value defined here as

$$\chi_j^2 = \sum_{k=1,i=1}^{M,N} \frac{[\Delta R_{np}^{exp}(k,i) - \Delta R_{np}^{th}(k,j)]^2}{[\delta\Delta R_{np}^{exp}(k,i)]^2}, \quad (1)$$

where $k = 1,2......M$ represent $^{48}$Ca, $^{64}$Ni, $^{124}$Sn, and $^{208}$Pb, respectively. $i = 1,2......N$, where $N$ is the number of adopted neutron skin thicknesses for nucleus $k$. $\Delta R_{np}^{th}(k,j)$ ($j = 1,2......28$) is the theoretical neutron skin thickness of nucleus $k$ corresponding to the effective interaction $j$. The randomly adopted effective interactions are Z, Es, E, Zs, Zs* [45], SIII [46], SkP [47], SkS1 [48], SkT6, SkT7 [49], RATP [50], SGII [51], SkS2 [48], SkM* [52], SLy4 [53], SkM [54], DD-ME2 [55], SkS3 [48], TW99 [56], PKO2, PKO3 [57], PKDD [58], PKO1 [59], PK1 [58], NL3 [60], NL-Z2 [61], NL-Z [62], and NL1 [63]. They are labeled with numbers from 1 to 28, respectively, as shown in Fig. 1. Each effective interaction corresponds to a specific $L$ value. These interactions cover a large $L$ range from approximately −50 to 140 MeV. $\Delta R_{np}^{exp}(k,i)$ and $\delta\Delta R_{np}^{exp}(k,i)$ are the $i$th experimental neutron skin thickness and error for nucleus $k$, respectively.

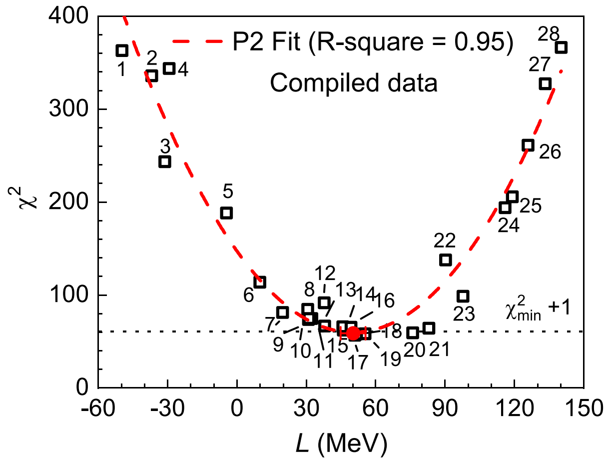


**Fig. 1.** (color online) Slope $L$ versus $\chi^2$ obtained by the compiled 49 model-dependent $\Delta R_{np}$ values of $^{48}$Ca, $^{64}$Ni, $^{124}$Sn, and $^{208}$Pb; see Table I in Ref. [27] for details on the $\Delta R_{np}$ data. The dashed line denotes the quadratic polynomial (P2) fit with an $R$-Square value of 0.95. The filled red circle with error bar represents the extracted $L$ result at the minimum $\chi^2$. The interaction parameter sets used are labeled with numbers 1 to 28; see text for details.

First, the 49 compiled model-dependent $\Delta R_{np}$ values of $^{48}$Ca, $^{64}$Ni, $^{124}$Sn, and $^{208}$Pb [27] are adopted to constrain $L$. These data are available in Table I in Ref. [27], which were obtained by various experiments; see Ref. [27] and references therein for details. The obtained $\chi^2$ as a function of $L$ is plotted in Fig. 1. In the $\chi^2$ calculations (Eq. (1)), only the reported experimental errors of neutron skins are considered. The scattering of the $\chi^2$ data points would be mainly caused by the difference of interaction models. Subsequently, the obtained $\chi^2$ as a function of $L$ is fitted by the quadratic polynomial (P2) function, namely, $\chi^2 = aL^2 + bL + c$. Then, an $L$ value of 50(6) MeV is deduced at the minimum $\chi^2$, $\chi^2_{min}$, via the P2 fit function. The final error of $L$ includes the uncertainties from fitting parameters and statistics. The $L$ uncertainty caused by fitting parameters mainly originates from the model difference. As shown in Fig. 1, the obtained $\chi^2_{min}$ value for the 49 $\Delta R_{np}$ is approximately 60. As a result, our normalized $\chi_n$ of $1.1\pm0.1$ is close to 1 within the error bar, which means that there are no significant unidentified systematic uncertainties. Therefore, similar to Ref. [42], the statistical error with a confidence level of 68.3% for the slope $L$ is obtained using the $\chi^2_{min}+1$ method.

Furthermore, we also constrain the slope $L$ using the so-called model-independent $\Delta R_{np}$ value of $^{48}$Ca and $^{208}$Pb determined by the CREX and PREX experiments [23, 33], as shown in Fig. 2. The obtained $L$ of 45(32) MeV is very consistent with the result of 50(6) MeV determined by the compiled model-dependent $\Delta R_{np}$ of $^{48}$Ca, $^{64}$Ni, $^{124}$Sn, and $^{208}$Pb [27]. The difference of their center values is only approximately 5 MeV, which demon-

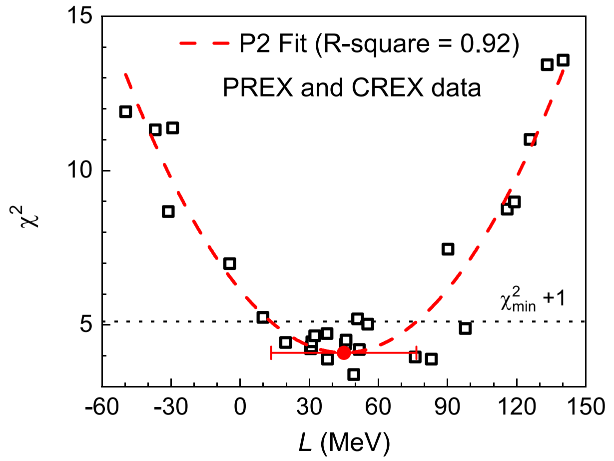


**Fig. 2.** (color online) Same as Fig. 1, but $\chi^2$ values are obtained by the two model-independent $\Delta R_{np}$ values from the CREX and PREX experiments [23, 33].

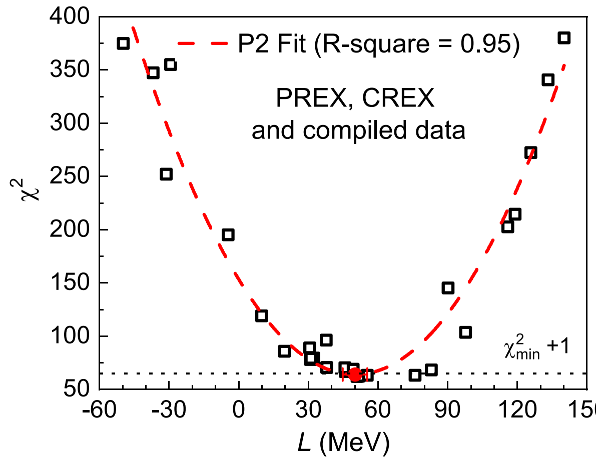


**Fig. 3.** (color online) Same as Fig. 1, but $\chi^2$ values are determined by all data used in Figs. 1 and 2.

strates the consistency of $\Delta R_{np}$ from different experiments.

Finally, in Fig. 3, the slope $L$ is constrained to be 50(6) MeV using all fifty-one $\Delta R_{np}$ values, including the model-dependent and -independent data used in Figs. 1 and 2. Figure 4 shows a comparison of the obtained $L$ in this work with the reported data from different observables and methodologies; see the review article in Ref. [14] and references therein for more details. Our $L$ result constrained by the abundant $\Delta R_{np}$ data from various experiments has high precision. In particular, our $L$ value is consistent with the so-called world-averaged result, namely, a weighted mean value of 57.2(22) MeV obtained using literature data, as shown in Fig. 4. Their difference is only approximately 7.2(64) MeV.

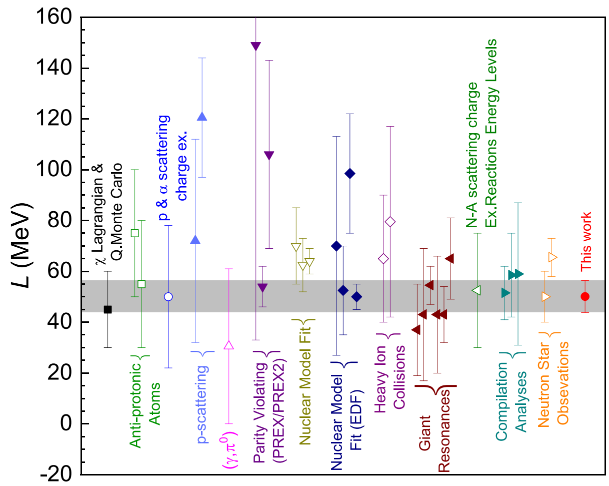


**Fig. 4.** (color online) Comparison of the $L$ value obtained in this study with the reported results from various methods, taken from Ref. [14]. The gray area indicates the uncertainty of our $L$.

## III. NEUTRON STAR RADIUS AND DISCUSSION

We further revisit the effects of our $L$ on the neutron star radii $R_{1.4}$ at 1.4 solar-mass (1.4 $M_\odot$). To easily understand the effects of the EoS parameters, the neutron star radii $R$ can be empirically expressed as [4]

$$R^4 \propto \frac{\rho^2}{3\rho_0}\left[\frac{K_0}{3}\left(\frac{\rho}{\rho_0}-1\right)+\frac{Q_0}{18}\left(\frac{\rho}{\rho_0}-1\right)^2+L\delta^2\right], \quad (2)$$

where $\delta=(\rho_n-\rho_p)/\rho$ is the asymmetry parameter, and $\rho_n$ and $\rho_p$ are the neutron and proton densities, respectively. The $R_{1.4}$-$L$ correlation deduced from various EoS parameter sets is relatively weak [4], and there is a model-dependent $R_{1.4}$ spread of approximately 2 km at one given $L$ [4, 15]. Consequently, as indicated by Eq. (2), the $L$ value alone is insufficient to characterize $R_{1.4}$.

However, the effects of $L$ on $R_{1.4}$ can be evaluated by adjusting the coupling constants associated with the vector-isovector meson $\rho$ in the relativistic mean-field Lagrangian, while the coupling strengths of isoscalar mesons are kept; for more details, see Ref. [5]. For instance, the linear $R_{1.4}$-$L$ relationships were established using such methods based on the TM1 and IUFSU EoS families [5]. Similarly, we also deduced the $R_{1.4}$-$L$ relationships from the DD-ME2 and TW99 EoS families. The matter in the core of a neutron star is composed of neutrons, protons, electrons, and muons and is assumed to be in $\beta$-equilibrium. For the core, we describe the EoS of uniform neutron star matter using the DD-ME2 and TW99 models. For the inner and outer crust regions, the EoSs of nonuniform matter are generated by the Thomas-Fermi approximation and Baym-Pethick-Sutherland, respectively. By fitting the deduced $R_{1.4}$-$L$ relationships (see Fig. 5) linear functions of $R_{1.4}=12.12+0.0189L$ and $R_{1.4}=11.03+0.0211L$ were obtained for the DD-ME2 and TW99 families, respectively. These linear functions are helpful to

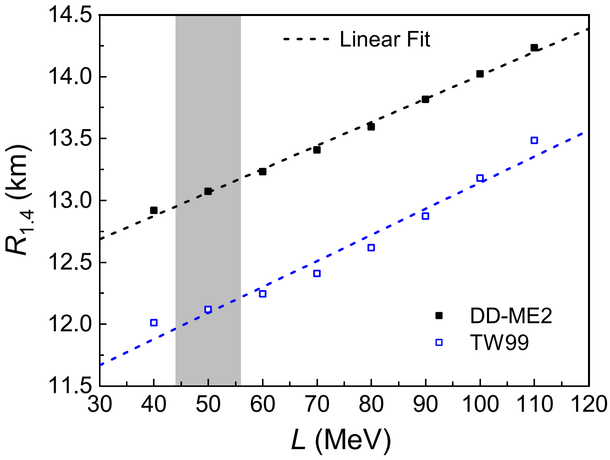


**Fig. 5.** (color online) $R_{1.4}$-$L$ correlations obtained by the DD-ME2 and TW99 EoS families. The dashed lines show the linear fit curves. The shaded area is the range of $L$ constrained by this study.

evaluate the effects of $L$ on the $R_{1.4}$ determinations. The spread of 30−110 MeV for $L$ leads to an $R_{1.4}$ uncertainty of approximately 1.6 km under the same theoretical framework (see Fig. 5). This is comparable to the model-dependent $R_{1.4}$ uncertainty of approximately 2 km for the different EoS families [4, 15]. Compared to the $R_{1.4}$ uncertainty of approximately 1.6 km caused by the $L$ spread of 30−110 MeV, the obtained $L$ of 50(6) MeV in this study from the finite nucleus system improves the $R_{1.4}$ precision (resulted only by $L$) by a factor of approximately 7 to be around 0.24 km under the same theoretical framework (see Fig. 5). Therefore, at the precision level of our $L$, the model-dependent $R_{1.4}$ uncertainty of approximately 2 km becomes more obvious [4, 15]. Furthermore, as shown in Fig. 5, there is an obvious model-dependent $R_{1.4}$ difference of approximately 1 km between the DD-ME2 and TW99 EoS families. For the model-dependent $R_{1.4}$ difference between the TM1 and IUFSU EoS families, as shown in Fig. 15 in Ref. [5], which was explained by the difference of incompressibility coefficient $K_0$ [5], the $Q_0$ value of −285 MeV for the TM1 is very close to that of −290 MeV for the IUFSU EoS family [15]. Compared to $K_0$ and $L$, the poorly understood $Q_0$ has a large spread from ~ −1000 to ~ 1000 MeV [15]. We note that the DD-ME2 and TW99 families have almost the same $K_0$, but the $Q_0$ values are completely different: 478 MeV and −544 MeV, respectively [15]. Therefore, it would also be interesting to further study the $R_{1.4}$ deviation caused by the poorly understood $Q_0$ using the DD-ME2 and TW99 EoS families. Besides, $K_0$ and $Q_0$ largely influence the high-density behaviors of EoSs and the magnitude of $R_{1.4}$ of neutron stars.

## IV. SUMMARY

The symmetry energy slope $L$ at the saturation density was constrained by neutron skins from various experiments. The determined $L$ of 50(6) MeV is consistent with the so-called world-averaged result from different observables and methodologies. Furthermore, based on the DD-ME2 and TW99 EoS families, the linear $R_{1.4}$-$L$ relationships were established to study the effects of the newly constrained $L$ on the radius determinations of 1.4 solar-mass neutron stars. Significant model-dependence of neutron star radius was observed as a result of varying skewness parameter $Q_0$. Our $L$ value effectively reduces the $R_{1.4}$ uncertainty of neutron stars caused by the $L$ spread by a factor of approximately 7 to be around 0.24 km under the same theoretical framework, which is smaller than the uncertainty of approximately 2 km from the different EoS families.

## ACKNOWLEDGEMENTS

*We would like to thank J. J. Li for the useful discussions and calculations.*

## References

[1] B. Li, L. Chen, and C. Ko, Phys. Rep. **464**, 113 (2008)
[2] J. M. Lattimer and M. Prakash, Science **304**, 536 (2004)
[3] J. M. Lattimer and M. Prakesh, Phys. Rep. **442**, 109 (2007)
[4] N. Alam, B. K. Agrawal, M. Fortin *et al.*, Phys. Rev. C **94**, 052801(R) (2016)
[5] J. Hu, S. Bao, Y. Zhang *et al.*, Prog. Theor. Exp. Phys. **2020**, 043D01 (2020)
[6] B.-A. Li and M. Magno, Phys. Rev. C **102**, 045807 (2020)
[7] B.-A. Li, B.-J. Cai, W.-J. Xie *et al.*, Universe **7**, 182 (2021)
[8] J. Richter and B.-A. Li, Phys. Rev. C **108**, 055803 (2023)
[9] K. Huang, H. Shen, J. Hu, and Y. Zhang, Phys. Rev. C **109**, 045804 (2024)
[10] X. Viñas, P. Bano, Z. Naik *et al.*, Symmetry **16**, 215 (2024)
[11] U. Garg and G. Colò, Prog. Part. Nucl. Phys. **101**, 55 (2018)
[12] S. Shlomo, V. M. Kolomietz, and G. Colò, Eur. Phys. J. A **30**, 23 (2006)
[13] Z. Z. Li, Y. F. Niu, and G. Colò, Phys. Rev. Lett. **131**, 082501 (2023)
[14] H. Sotani, N. Nishimura, and T. Naito, Prog. Theor. Exp. Phys. **2022**, 041D01 (2022)
[15] B. Sun, S. Bhattiprolu, and J. M. Lattimer, Phys. Rev. C **109**, 055801 (2024)
[16] B. A. Brown, Phys. Rev. Lett. **85**, 5296 (2000)
[17] M. von Schmid, T. Aumann, S. Bagchi *et al.*, Eur. Phys. J. A **59**, 83 (2023)
[18] J. T. Zhang, P. Ma, Y. Huang *et al.*, Phys. Rev. C **108**, 014614 (2023)
[19] K. Yue, J. T. Zhang, X. L. Tu *et al.*, Phys. Rev. C **100**, 054609 (2019)
[20] Y. Huang, S. Y. Xia, Y. F. Li *et al.*, Phys. Lett. B **856**, 138902 (2024)
[21] Y. Huang, L. Xayavong, X. L. Tu *et al.*, Phys. Lett. B **847**,

138293 (2023)
[22] A. Trzcińska, J. Jastrzebski, P. Lubiński *et al*., Phys. Rev. Lett. **87**, 082501 (2001)
[23] D. Adhikari, H. Albataineh, D. Androic *et al*., Phys. Rev. Lett. **126**, 172502 (2021)
[24] G. A. Korolev, A. V. Dobrovolsky, A. G. Inglessi *et al*., Phys. Lett. B **780**, 200 (2018)
[25] M. Tanaka, M. Takechi, A. Homma *et al*., Phys. Rev. Lett. **124**, 102501 (2020)
[26] S. Terashima, H. Sakaguchi, H. Takeda *et al*., Phys. Rev. C **77**, 024317 (2008)
[27] J. T. Zhang, X. L. Tu, P. Sarriguren *et al*., Phys. Rev. C **104**, 034303 (2021)
[28] G. D. Alkhazov, M. N. Andronenko, A. V. Dobrovolsky *et al*., Phys. Rev. Lett. **78**, 2313 (1997)
[29] I. Tanihata, H. Hamagaki, O. Hashimoto *et al*., Phys. Rev. Lett. **55**, 2676 (1985)
[30] A. Krasznahorkay, M. Fujiwara, P. van Aarle *et al*., Phys. Rev. Lett. **82**, 3216 (1999)
[31] H. Sagawa, S. Yoshida, X.-R. Zhou *et al*., Phys. Rev. C **76**, 024301 (2007)
[32] J. Jastrzebski, A. Trzcińska, P. Lubiński *et al*., Int. J. Mod. Phys. E **13**, 343 (2004)
[33] D. Adhikari, H. Albataineh, D. Androic *et al*., Phys. Rev. Lett. **129**, 042501 (2022)
[34] P.-G. Reinhard, X. Roca-Maza, and W. Nazarewicz, Phys. Rev. Lett. **129**, 232501 (2022)
[35] C. Mondal and F. Gulminelli, Phys. Rev. C **107**, 015801 (2023)
[36] T. Miyatsu, M.-K. Cheoun, K. Kim *et al*., Phys. Lett. B **843**, 138013 (2023)
[37] T.-G. Yue, Z. Zhang, and L.-W. Chen, arXiv: 2406.03844v1
[38] Z. Zhang and L.-W. Chen, Phys. Rev. C **108**, 024317 (2023)
[39] F. Sammarruca, Symmetry **16**, 34 (2024)
[40] J. M. Lattimer, Particles **6**, 30 (2023)
[41] B. T. Reed, F. J. Fattoyev, C. J. Horowitz *et al*., Phys. Rev. Lett. **126**, 172503 (2021)
[42] Z. Zhang and L.-W. Chen, Phys. Lett. B **726**, 234 (2013)
[43] L.-W. Chen, C. M. Ko, B.-A. Li *et al*., Phys. Rev. C **82**, 024321 (2010)
[44] X. Roca-Maza, M. Centelles, X. Viñas *et al*., Phys. Rev. Lett. **106**, 252501 (2011)
[45] J. Friedrich and P.-G. Reinhard, Phys. Rev. C **33**, 335 (1986)
[46] M. Beiner, H. Flocard, N. Van Giai *et al*., Nucl. Phys. A **238**, 29 (1975)
[47] J. Dobaczewski, H. Flocard, and J. Treiner, Nucl. Phys. A **422**, 103 (1984)
[48] J. Gómez, C. Prieto, and J. Navarro, Nucl. Phys. A **549**, 125 (1992)
[49] F. Tondeur, M. Brack, M. Farine *et al*., Nucl. Phys. A **420**, 297 (1984)
[50] M. Rayet, M. Arnould, G. Paulus *et al*., Astron. Astrophysics. **116**, 183 (1982)
[51] N. Van Giai and H. Sagawa, Phys. Lett. B **106**, 379 (1981)
[52] J. Bartel, P. Quentin, M. Brack *et al*., Nucl. Phys. A **386**, 79 (1982)
[53] E. Chabanat, P. Bonche, P. Haensel *et al*., Nucl. Phys. A **635**, 231 (1998)
[54] H. Krivine, J. Treiner, and O. Bohigas, Nucl. Phys. A **336**, 155 (1980)
[55] G. A. Lalazissis, T. Nikšić, D. Vretenar *et al*., Phys. Rev. C **71**, 024312 (2005)
[56] S. Typel and H. H. Wolter, Nucl. Phys. A **656**, 331 (1999)
[57] W. Long, H. Sagawa, J. Meng *et al*., Europhys. Lett. **82**, 12001 (2008)
[58] W. Long, J. Meng, N. Van Giai *et al*., Phys. Rev. C **69**, 034319 (2004)
[59] W.-H. Long, N. Van Giai, and J. Meng, Phys. Lett. B **640**, 150 (2006)
[60] G. A. Lalazissis, J. König, and P. Ring, Phys. Rev. C **55**, 540 (1997)
[61] M. Bender, K. Rutz, P.-G. Reinhard *et al*., Phys. Rev. C **60**, 034304 (1999)
[62] M. Rufa, P.-G. Reinhard, J. A. Maruhn *et al*, Phys. Rev. C **38**, 390 (1988)
[63] P. Reinhard, M. Rufa, J. Maruhn *et al*., Z. Phys. A **323**, 13 (1986)